

CIRJE-F-917

**A New Improvement Scheme for Approximation Methods of
Probability Density Functions**

Akihiko Takahashi
The University of Tokyo

Yukihiro Tsuzuki
Graduate School of Economics, The University of Tokyo

February 2014; Revised in August 2014

CIRJE Discussion Papers can be downloaded without charge from:

<http://www.cirje.e.u-tokyo.ac.jp/research/03research02dp.html>

Discussion Papers are a series of manuscripts in their draft form. They are not intended for circulation or distribution except as indicated by the author. For that reason Discussion Papers may not be reproduced or distributed without the written consent of the author.

A New Improvement Scheme for Approximation Methods of Probability Density Functions *

Akihiko Takahashi[†], Yukihiro Tsuzuki[‡]

August 22, 2014

Abstract

This paper develops a new scheme for improving an approximation method of a probability density function, which is inspired by the idea in *the Hilbert space projection theorem*. Moreover, we apply “Dykstra’s cyclic projections algorithm” for its implementation. Numerical examples for application to an asymptotic expansion method in option pricing demonstrate the effectiveness of our scheme under SABR model.

Keywords: Density approximation, Probability density function, Asymptotic expansion, Best approximation in inner product spaces, Dykstra’s algorithm, Option pricing, SABR model

*Forthcoming in **Journal of Computational Finance**. All the contents expressed in this research are solely those of the authors and do not represent the view of any institutions. The authors are not responsible or liable in any manner for any losses and/or damages caused by the use of any contents in this research.

[†]Graduate School of Economics, University of Tokyo

[‡]Graduate School of Economics, University of Tokyo, E-mail: yukihirotsuzuki@gmail.com

1 Introduction

An approximation for a probability density function is a very interesting topic in various research fields. In fact, it seems so useful that a precise analytical approximation for a density would lead to substantial reduction of computational burden so that the subsequent analyses could be very easily implemented. Particularly, in finance the approximations for the densities of the asset prices have drawn much attention for at least more than two decades since fast and precise computation is so important in terms of competition and risk management, which is crucial in the derivatives business.

Examples among a large number of the related researches are Bayer and Laurence [1], Fouque, Papanicolaou and Sircar [5], Hagan, Kumar, Lesniewski, and Woodward [7], Gatheral, Hsu, Laurence, Ouyang, and Wang [6], Siopacha and Teichmann [11] and an asymptotic expansion approach ([12], [9], [10], [13]). Although those approximation methods have been successfully applied in practice, there are still some rooms for improvement. For example, it is well known that while the density of the approximation formula for SABR model ([7]) provides sufficiently accurate approximations for option pricing, it has the negative values for the left tail, which could create an arbitrage opportunity in option trading.

This paper develops a new scheme for improving density approximation methods, which also provides precise approximations of option values. Specifically, our scheme is inspired by the idea in *the Hilbert space projection theorem* and the so called “Dijkstra’s cyclic projections algorithm” is applied for its implementation. We also remark that our scheme can be easily implemented in practice, where we need only market data for usual calibration such as option prices with strikes.

We firstly note that our scheme can start with any given approximate density. Then, we improve the density so that it meets a set of conditions such as the non-negativity and the total mass being one that the density function must satisfy. Moreover, based on our method it becomes possible to create a new approximate density to possess certain properties desirable in practice such as calibration to the market forward and option prices. In addition, the method enable a new density to incorporate known information if any, such as the decreasing speed of the tails of the true density. In this manner, we develop a generic scheme which achieves the improvement of the approximation, whatever a starting approximate density is.

Next, let us remark on the criteria on improvement of a density approximation. In general, as the criteria vary such that an improved density provides more accurate ATM option prices, nonnegative prices or butterfly spreads and so on, they are inevitably subjective. For instance, which is the better is not definite between

- (1) approximation which excludes negative butterfly spreads
- (2) approximation which produces prices close to model prices around ATM, but admits negative butterfly spreads.

For example, Doust [4] is a kind of the first, while [7] is of the second. As for our method, it guarantees the first criterion (non-negativity of butterfly spreads) together with our best effort at the second one (accuracy for model prices). Consequently, the method is robust with respect to the first criterion. In terms of the second criterion, although the accuracy depends on a starting approximation, our method is still robust with a decent initial approximation.

Furthermore, numerical experiments for vanilla option pricing under SABR model demonstrate the validity of our scheme. In fact, with few additional computational costs our scheme improves the third and fifth order asymptotic expansion preserving the required conditions such as nonnegative densities under an appropriate forward measure.

We finally remark that our scheme is general and flexible enough to include a set of conditions and information as one would like to put on an approximate density, and it can be applied to approximation methods other than the asymptotic expansion method. For example, a number of researches have been going on in order to extend SABR model with fixing the problem of the negative densities in the method of [7]. (For instance, see [4].) We note that our scheme is also a candidate for handling this issue. Also,

the estimate of the absorption probability based on Monte Carlo simulations as in [4] can be consistently reflected in our scheme.

The organization of the paper is as follows: After the next section describes the setup of the problem, Section 3 provides a concrete formulation of our method as well as the algorithm for the implementation. Section 4 shows numerical examples under SABR model. Section 5 concludes.

2 Setup

Let S_t be the spot price of the underlying asset at time $t \in [0, T]$ and consider a density f of S_T , where S_T takes a value in $I \subseteq \mathbb{R}$, such as $I = \mathbb{R}$, $[0, +\infty)$ or $(0, +\infty)$. Clearly, the density function f of the price S_T must satisfy the following property. Hereafter, η stands for a density function under a risk-neutral or an appropriate forward probability measure.

Property 1. (*Density Condition*) : for a function η on $I \subseteq \mathbb{R}$,

(1) $\int_I \eta(x) dx = 1$

(2) $\eta \geq 0$ a.e.

Suppose that we have an approximation \tilde{f} of the density function f based on a certain method. Note that the approximation \tilde{f} does not necessarily have Property 1. Also, the forward price is usually given independently of models, and hence the average value of the underlying asset price at T should be equal to the given forward price with maturity T .

Moreover, it is known that some approximation formulas (e.g. the asymptotic expansion method) provides rather precise approximations for the values close to At-The-Money(ATM) options. Thus, it is reasonable that the option prices around ATM under a new approximate density function are calibrated to those computed based on an initial approximation formula, and that a new density is equal to the one obtained by the approximation formula for a certain range of the underlying asset price around ATM. We call those properties by *Calibration Condition*:

Property 2. (*Calibration Condition*)

(3) $\int_I x \eta(x) dx = S_0$

(4) $\int_I (x - K_n)_+ \eta(x) dx = C_{K_n}$ for some given strikes $\{K_n\}_{n=1}^N$

(5) $\eta = \tilde{f}$ on some subset I_0 of I

Here, the risk-free interest rate as well as the dividend rate of the underlying asset are assumed to be zero for simplicity. C_{K_n} denotes the option price with strike K_n and maturity T computed by the initial approximation formula.

In contrast to the accuracy around ATM, the values of the approximated density \tilde{f} may not be reliable around deep out of the money. However, how fast a density decreases to zero is known under some models or through a moment formula for the implied volatility. Namely, the following quantities are known:

$$\tilde{p} := \sup\{p > 0 : \mathbb{E}S_T^p < +\infty\} \tag{2.1}$$

$$\tilde{q} := \sup\{q > 0 : \mathbb{E}S_T^{-q} < +\infty\} \tag{2.2}$$

under some models or through the moment formula derived by Lee [8]:

$$\tilde{p} = \frac{1}{2\beta_R} + \frac{\beta_R}{8} + \frac{1}{2}, \quad \tilde{q} = \frac{1}{2\beta_L} + \frac{\beta_L}{8} - \frac{1}{2}, \tag{2.3}$$

where

$$\beta_R := \limsup_{x \rightarrow +\infty} \frac{IV^2(x)}{|x|/T}, \quad (2.4)$$

$$\beta_L := \limsup_{x \rightarrow -\infty} \frac{IV^2(x)}{|x|/T}. \quad (2.5)$$

Here, $IV(x)$ is an implied volatility function in terms of the log-moneyness that is, $x = \log(S_0/K)$.

Now, let us assume that \tilde{p} and \tilde{q} are known, and suppose $\chi : I \rightarrow (0, +\infty)$ be a density function which has the same order of the tail condition as f :

$$\int_{S_0}^{+\infty} x^p \chi(x) dx < +\infty \quad (p < \tilde{p}), \quad \int_0^{S_0} x^{-q} \chi(x) dx < +\infty \quad (q < \tilde{q}). \quad (2.6)$$

Then, it seems natural to impose the following condition:

Property 3. (*Tail Condition*)

(6) η has the same tail slopes as χ .

However, for ease of computation, the condition may be replaced with the following:

Property 4. (*Weak Tail Condition*)

(6-1) $\eta \leq \chi$ on $(0, K_L]$ for some positive number K_L

(6-2) $\eta \leq \chi$ on $[K_R, +\infty)$ for some positive number K_R

Thus, we state our problem formally as follows:

Definition 1 (Problem). Find a new approximate density function f^* for the target density f such that it satisfies the properties 1, 2 and 4, and

$$\|f - f^*\| \leq \|f - \tilde{f}\|, \quad (2.7)$$

where \tilde{f} is a given approximation of the density function of f , and the norm $\|\cdot\|$ will be defined based on the inner product (3.1) in the next section.

3 Formulation and Algorithm

This section concretely formulates the previous discussion and provides an algorithm for the implementation.

3.1 Formulation

Firstly, suppose a probability space $(\mathbb{R}, \mathcal{M}, \mu)$, where \mathcal{M} is a set of all Lebesgue measurable subsets of \mathbb{R} , the measure μ is assumed to have a density which is equal to χ given in the previous section on I and to 0 on I^c , the complement of I . Next, we define a Hilbert space $\mathcal{H} = L^2(\mathbb{R}, \mathcal{M}, \mu)$, that is the set of square integrable functions on $(\mathbb{R}, \mathcal{M}, \mu)$ equipped with the inner product:

$$\langle f, g \rangle = \int_I f(x)g(x)\chi(x)dx \text{ for } f, g \in \mathcal{H}. \quad (3.1)$$

Hereafter, roughly speaking, the density function denoted by f in Definition 1 is to be estimated by means of projecting $\varphi = f/\chi$ onto a subspace of \mathcal{H} as φ^* , and then considering $f^* = \varphi^*\chi$.

Let us define some subsets of \mathcal{H} as \mathcal{K}_D , \mathcal{K}_C and \mathcal{K}_T which stand for (1)-(2) in **Property 1**, (3)-(5) in **Property 2** and (6-1)-(6-2) in **Property 4** defined in Section 2, respectively:

$$\mathcal{K}_D := \{\varphi \in \mathcal{H} \mid \langle \varphi, 1_I \rangle = 1\} \cap \bigcap_{x \in I} \{\varphi \in \mathcal{H} \mid \langle \varphi, \delta_x \rangle \geq 0\}, \quad (3.2)$$

$$\mathcal{K}_C := \{\varphi \in \mathcal{H} \mid \langle \varphi, id_I \rangle = S_0\} \cap \bigcap_{n \leq N} \{\varphi \in \mathcal{H} \mid \langle \varphi, g_{K_n} \rangle = C_{K_n}\} \cap \bigcap_{x \in I_0} \{\varphi \in \mathcal{H} \mid \langle \varphi, \delta_x \rangle = \tilde{f}(x)\} \quad (3.3)$$

and

$$\mathcal{K}_T := \bigcap_{x \in (0, K_L]} \{\varphi \in \mathcal{H} \mid \langle \varphi, \delta_x \rangle \leq \chi(x)\} \cap \bigcap_{x \in [K_R, +\infty)} \{\varphi \in \mathcal{H} \mid \langle \varphi, \delta_x \rangle \leq \chi(x)\}. \quad (3.4)$$

Here 1_I , id_I and g_{K_n} are elements of \mathcal{H} such that $1_I(x) = 1$, $id_I(x) = x$ and $g_{K_n}(x) = (x - K_n)_+$. Moreover, S_0 is the initial value of the underlying asset, C_{K_n} denotes the option price with strike K_n and maturity T (defined in **Property 2**-(4)) and I_0 is a subset of I in which S_T takes a value. In addition, \tilde{f} is a given approximate density which we can choose arbitrarily.

Moreover, let us define \mathcal{K} as the intersection of \mathcal{K}_D , \mathcal{K}_C and \mathcal{K}_T :

$$\mathcal{K} := \mathcal{K}_D \cap \mathcal{K}_C \cap \mathcal{K}_T, \quad (3.5)$$

We assume \mathcal{K} is nonempty, which is expected to be mostly satisfied in practice, and is in fact satisfied for our numerical examples in Section 4.

Then, let $\tilde{\varphi} := \tilde{f}/\chi \notin \mathcal{K}$, and the best approximation set from $\tilde{\varphi}$ to \mathcal{K} is defined as

$$P_{\mathcal{K}}(\tilde{\varphi}) := \{\varphi^* \in \mathcal{K} \mid \|\tilde{\varphi} - \varphi^*\| = \inf_{\eta \in \mathcal{K}} \|\tilde{\varphi} - \eta\|\}. \quad (3.6)$$

Note that the set $P_{\mathcal{K}}(\tilde{\varphi})$ has the only one element since \mathcal{K} is a closed convex set in a Hilbert space. Hereafter, we may use the notation $P_{\mathcal{K}}(\tilde{\varphi})$ for the unique element of $P_{\mathcal{K}}(\tilde{\varphi})$ without any confusion.

Thus, due to the Hilbert space projection theorem, $P_{\mathcal{K}}(\tilde{\varphi})$ is a better approximation for $f/\chi \in \mathcal{K}$ than $\tilde{\varphi} := \tilde{f}/\chi \notin \mathcal{K}$. Namely,

$$\begin{aligned} \|f/\chi - P_{\mathcal{K}}(\tilde{\varphi})\|^2 &= \|f/\chi - \varphi^\perp\|^2 + \|\varphi^\perp - P_{\mathcal{K}}(\tilde{\varphi})\|^2 \\ &\leq \|f/\chi - \varphi^\perp\|^2 + \|\varphi^\perp - \tilde{\varphi}\|^2 \\ &= \|f/\chi - \tilde{\varphi}\|^2, \end{aligned} \quad (3.7)$$

where φ^\perp is the foot of a perpendicular line through $\tilde{\varphi}$ and $P_{\mathcal{K}}(\tilde{\varphi})$ from f/χ .

Consequently, we obtain a better approximated density function than the original one \tilde{f} as

$$f^* := P_{\mathcal{K}}(\tilde{\varphi})\chi. \quad (3.8)$$

That is, equivalently to (3.7), we have

$$\int_I |f(x) - f^*(x)|^2 \frac{1}{\chi(x)} dx \leq \int_I |f(x) - \tilde{f}(x)|^2 \frac{1}{\chi(x)} dx. \quad (3.9)$$

3.2 Algorithm

This subsection briefly describes a general iterative method called *Dijkstra's algorithm*. (See pp. 207-214 of Deutsch [3] for the detail of the algorithm and its convergence discussion.)

This method will be applied to computation of (3.6) in the numerical examples of Section 4.

Let $\tilde{\mathcal{K}}$ be a convex set, which is an intersection of finite many closed convex sets \mathcal{K}_i ($i = 1, 2, \dots, r$) in a Hilbert space \mathcal{H} :

$$\tilde{\mathcal{K}} = \bigcap_{i=1}^r \mathcal{K}_i. \quad (3.10)$$

Here, we assume $\tilde{\mathcal{K}}$ to be nonempty.

We remark that in our case described in Section 3.1, \mathcal{K}_i ($i = 1, 2, \dots, r$) correspond to the discretized versions of the convex sets in (3.2), (3.3) and (3.4). Thus, $\tilde{\mathcal{K}}$ is regarded as a discretization of \mathcal{K} defined in (3.5).

First, for each $n \in \mathbb{N}$, let $[n]$ denote $n \bmod r$; that is,

$$[n] := \{1, 2, \dots, r\} \cap \{n - kr : k = 0, 1, 2, \dots\}. \quad (3.11)$$

For instance, $[1] = 1, [2] = 2, \dots, [r] = r, [r+1] = 1, \dots, [2r] = r, \dots$

Next, for $\tilde{\varphi} \in \mathcal{H}$, set

$$\begin{aligned} \varphi_0 &:= \tilde{\varphi}, \quad e_{-(r-1)} = \dots = e_{-1} = e_0 = 0, \\ \varphi_n &:= P_{\mathcal{K}_{[n]}}(\varphi_{n-1} + e_{n-r}), \\ e_n &:= \varphi_{n-1} + e_{n-r} - \varphi_n \\ &= \varphi_{n-1} + e_{n-r} - P_{\mathcal{K}_{[n]}}(\varphi_{n-1} + e_{n-r}). \end{aligned} \quad (3.12)$$

Here, $P_{\mathcal{K}_{[n]}}(\varphi_{n-1} + e_{n-r})$ is defined as in Eq.(3.6). Namely,

$$P_{\mathcal{K}_{[n]}}(\varphi_{n-1} + e_{n-r}) := \{\varphi^* \in \mathcal{K}_{[n]} \mid \|\varphi_{n-1} + e_{n-r} - \varphi^*\| = \inf_{\eta \in \mathcal{K}_{[n]}} \|\varphi_{n-1} + e_{n-r} - \eta\|\}. \quad (3.13)$$

Then, it is the best approximation from $\varphi_{n-1} + e_{n-r}$ to the convex set $\mathcal{K}_{[n]}$ which is one of \mathcal{K}_i ($i = 1, 2, \dots, r$).

Finally, we obtain the following convergence result based on the Boyle-Dykstra theorem:

$$\lim_{n \rightarrow +\infty} \|\varphi_n - P_{\mathcal{K}}(\tilde{\varphi})\| = 0. \quad (3.14)$$

See Theorem 9.24 in p. 213 of Deutsch [3] for the Boyle-Dykstra theorem and its proof.

We remark that in our case in Section 3.1, the convergence holds for $\tilde{\varphi}$ defined by any \tilde{f} and χ as $\tilde{\varphi} = \tilde{f}/\chi$.

3.3 Implementation

This subsection describes how to implement our scheme numerically. More details specific to models will be explained in Section 4.

In principle, it is so simple to implement our scheme just in order to meet the conditions (1)-(2) in **Property 1**, (3)-(5) in **Property 2** and (6-1)-(6-2) in **Property 4**. Although some knacks are recommended in what follows to make the procedure stable and to get a more desirable result, our method itself guarantees a new approximate density to satisfy the above conditions independently of these knacks.

Choice of a Hilbert space Our scheme works on every Hilbert space theoretically. However, how to choose a Hilbert space, namely how to choose χ as a kernel of a Hilbert space, is crucial from a viewpoint of numerical implementation.

Specifically, we choose the kernel function χ of the Hilbert space as a function close to the target density function f as much as possible. In particular, we set χ as follows:

$$\chi := f_L 1_{(0, K_L)} + \tilde{f} 1_{[K_L, K_R)} + f_R 1_{[K_R, +\infty)}. \quad (3.15)$$

In this definition, \tilde{f} is a starting approximation for the density function f , and note that we may choose an arbitrary approximate density as \tilde{f} . In addition, f_L and f_R are some functions which have the similar tail behaviors as f . Here, K_L and K_R are chosen such that \tilde{f} is accurate on $[K_L, K_R)$.

In this Hilbert space the best approximation $P_{\mathcal{K}}(\tilde{\varphi})$ is expected to be close to 1_I , which makes the algorithm more stable. This is because if $\tilde{\varphi}$ is far from 1_I , an orthogonal projection of $\tilde{\varphi}$ onto the set $\{\varphi \in \mathcal{H} \mid \langle \varphi, 1_I \rangle = 1\}$ can violate the condition $\bigcap_{x \in I} \{\varphi \in \mathcal{H} \mid \langle \varphi, \delta_x \rangle \geq 0\}$.

This can be easily understood, if a two-dimensional case is considered: for instance, compare two projections from points $(1, 1)$ and $(2, 0)$ onto a convex set $\{(x, y) \in \mathbb{R}^2 \mid x + y = 1, x \geq 0, y \geq 0\}$. The algorithm (3.12) starting with a projection onto a plane $\{(x, y) \in \mathbb{R}^2 \mid x + y = 1\}$ converges after one iteration if the initial point is $(1, 1)$. On the other hand, the projected point from $(2, 0)$ is outside the convex set and more iterations are required.

In this framework, the norm to measure the accuracy is given by Eq.(3.9), which implies that more weights are put on tails. This norm is reasonable, because an original approximation is usually rather accurate around ATM and the purpose for using our scheme is to improve accuracy on tails.

Discretization For numerical implementation, we have to make the problem finite dimensional. Let us take a finite increasing sequence $\{x_i\}_{i=0}^d \subseteq \mathbb{R}$. Then, we can regard the Hilbert space \mathcal{H} as a d -dimensional vector space with an inner product:

$$\langle f, g \rangle = \sum_{i=1}^d f(x_i)g(x_i)\chi(x_i)(x_i - x_{i-1}). \quad (3.16)$$

If we choose $\{1_{[x_{i-1}, x_i)}\}_{i=1}^d$ as an orthogonal basis, an element $f \in \mathcal{H}$ can be identified with $(f(x_1), \dots, f(x_d)) \in \mathbb{R}^d$. The properties (1) to (5), (6-1) and (6-2) in Section 2 are conditions that an element $\eta/\chi \in \mathcal{H}$ is on a hyper-plane or on a half-space in a d -dimensional vector space. Projection of an element φ of \mathcal{H} onto a hyper-plane or a half-space \mathcal{N} is given by

$$P_{\mathcal{N}}(\varphi) = \varphi - \frac{1}{\|\varphi^*\|^2} (\langle \varphi, \varphi^* \rangle - c) \varphi^*, \quad (3.17)$$

if \mathcal{N} is a hyper-plane defined by $\mathcal{N} := \{\varphi \in \mathcal{H} \mid \langle \varphi, \varphi^* \rangle = c\}$ for some $\varphi^* \in \mathcal{H}$ and $c \in \mathbb{R}$, or

$$P_{\mathcal{N}}(\varphi) = \varphi - \frac{1}{\|\varphi^*\|^2} (\langle \varphi, \varphi^* \rangle - c)_+ \varphi^*, \quad (3.18)$$

if \mathcal{N} is a half space defined by $\mathcal{N} := \{\varphi \in \mathcal{H} \mid \langle \varphi, \varphi^* \rangle \leq c\}$. In both cases, these calculations are easy to implement and take little computational cost. After repeating the algorithm (3.12), we obtain the best approximation value at each point: $\{P_{\mathcal{K}}(\tilde{\varphi})(x_i)\chi(x_i)\}_{i=1}^d$. Finally, in order to calculate an option value with payoff g_K , we resort to a numerical integration:

$$\sum_{i=1}^d g_K(x_i) P_{\mathcal{K}}(\tilde{\varphi})(x_i) \chi(x_i) (x_i - x_{i-1}). \quad (3.19)$$

Procedure In summary, we have the following procedures:

1. Choose an increasing sequence $\{x_i\}_{i=0}^d \subseteq \mathbb{R}$ for discretization.
2. Calculate values of the given approximated function \tilde{f} at each point $\{x_i\}_{i=0}^d$.
3. Set a density function χ of a Hilbert space:
 - Choice of K_L and K_R is dependent on the domain where the original approximated function \tilde{f} is accurate. Please see Section 4 for the concrete examples of those choices.
 - For a left/right-tail behavior, it is natural to impose constrains such that the density function decreases to zero as $x \rightarrow 0$ and $x \rightarrow +\infty$.
More concretely, the tail of χ is set as $e^{-\frac{1}{2}(\log x)^2}$ or x^p for some p according to its decreasing speed.
In addition, χ should be a natural extension of \tilde{f} so that χ is continuous and decreases so fast to zero as the function \tilde{f} does around K_L and K_R .
4. Execute Dykstra's algorithm:
 - The algorithm (3.12) with an initial value \tilde{f}/χ^1 is iterated for $n = 1, \dots, N$. Please see Section 4 on how to determine N .
Each projection is calculated by Eq.(3.17) for a hyper-plane or Eq.(3.18) for a half space. It consists of finitely many operations in a finite dimensional vector space.
 - As a result, a set of values for the best approximation $\{P_{\mathcal{K}}(\tilde{\varphi})(x_i)\}_{i=0}^d$ is obtained.
5. Calculate option values:
 - Computation is executed numerically based on Eq.(3.19).

4 Numerical Example

4.1 Preparation

This section examines the validity of our scheme through numerical experiments by applying it to an asymptotic expansion method [13] under SABR model, where the dynamics of the underlying price process under a forward measure is expressed as follows:

$$\begin{aligned} dS_t &= \sigma_t S_t^c dW_t^1, \\ d\sigma_t &= \varepsilon \sigma_t dW_t^2. \end{aligned} \quad (4.1)$$

Here, $\varepsilon > 0$, $c \in (0, 1]$ and W^1 and W^2 are Brownian motions with a constant correlation ρ . In the numerical experiment, let us concentrate on the case of $0 < c < 1$.² In this case, it is well known that S_T can reach 0 with positive probability. According to the result by Benaim et al. [2], it holds that

$$\tilde{p} = +\infty, \quad \tilde{q} = 0, \quad (4.2)$$

where \tilde{p} and \tilde{q} are defined in (2.1). Then, while the density decreases so fast to zero on the right tail, the left tail is so fat that any moment is infinite: $\mathbb{E}(S_T^p) < +\infty$ for $p > 0$ and $\mathbb{E}(S_T^{-q}) = +\infty$ for $q > 0$.

Thus, taking this observation into account, it is reasonable to specify χ given in (3.15) as the following equations in $I := [0, +\infty)$:

$$\chi(x) = \begin{cases} A_L & x = 0, \\ \gamma x & x \in (0, K_L) \\ \tilde{f}(x) & x \in [K_L, K_R) \\ A_R \frac{1}{\sqrt{2\pi}} \frac{1}{x\tilde{\sigma}\sqrt{T}} e^{-\frac{(\log x - m)^2}{2\tilde{\sigma}^2 T}} & x \in [K_R, +\infty), \end{cases} \quad (4.3)$$

¹Alternatively, $\chi/\chi(\equiv 1)$ can be used in order not to take ill behaviors of \tilde{f} outside $[K_L, K_R)$ into account.

²The result for case of $c = 1$ with $\rho < 0$ will be given upon request.

where A_L is a positive constant and $m = \log S_0 - \frac{1}{2}\tilde{\sigma}^2 T$ with a positive value $\tilde{\sigma}$. The selection of the functions for $x = 0$, $x \in [0, K_L)$ and $x \in [K_R, +\infty)$ corresponds to Property 4 (*Weak Tail Condition*) in Section 2 and is reflected in \mathcal{K}_T in Section 3. On the other hand, $\tilde{f}(x)$ in $x \in [K_L, K_R)$ is obtained by the asymptotic expansion method, which provides rather precise approximations for the option values around ATM. It corresponds to **Property 2** (*Calibration Condition*) in Section 2 and is reflected in \mathcal{K}_C in Section 3.

With this setup, we calculate option prices by the following methods:

- (a) Monte Carlo simulation (Benchmark)
- (b) asymptotic expansion up to the fifth order
- (c) asymptotic expansion up to the third order
- (d) our algorithm with $K_n \in (K_L, K_R)$, $n = 1, \dots, N$ in **Property 2** (*Calibration Condition*) and with $f^* = \tilde{f}$ on $I_0 = [K_L, K_R)$. Here, \tilde{f} is obtained by the fifth order expansion as in (b) or by the third order expansion as in (c).

In the asymptotic expansion method, we consider the following perturbed SDE of (4.1) with a perturbation parameter δ , and expand it around $\delta = 0$ up to certain orders (that is, up to the fifth order in (b) and up to the third order in (c)) in order to obtain approximate densities of S_T .

$$\begin{aligned} dS_t^{(\delta)} &= \delta\sigma_t^{(\delta)}(S_t^{(\delta)})^c dW_t^1, \\ d\sigma_t^{(\delta)} &= \delta\varepsilon\sigma_t^{(\delta)} dW_t^2. \end{aligned} \tag{4.4}$$

Particularly, its first order approximate density is obtained as a normal density. Please see [9], [10] and [13] for the details of the computational method and applications. We remark that the method in [4] may be regarded within a class of an asymptotic expansion method, though its derivation is different from the one of the expansion used in this paper and references above.

As numerical experiments, we examine three cases of the parameter setting listed in Table 1. We remark that **Case 3** is the same as in Figure 4 of [4].

The parameters in (4.3) are specified in the following manner. Particularly, the choices of K_R and K_L are determined based on the discrepancies between the benchmark prices obtained by (a) Monte Carlo and the approximate prices obtained by (b) the fifth order expansion or (c) the third order expansion³. More precisely, K_R and K_L are set as a slightly lower price (for K_R) and a slightly higher price (for K_L) than strike prices where the discrepancies become relatively larger. We note that this procedure is not a tough task at all in practice.

1. We set $K_R = 120$ and $K_L = 0$ for **Case 1**, while $K_R = 132$ and $K_L = 72$ for **Case 2**. In **Case 3**, we set $K_R = 7.2224$ and $K_L = 2.3424$ for (b) the fifth order expansion and $K_R = 5.856$ and $K_L = 3.904$ for (c) the third order expansion.

Particularly for **Case 2** and **Case 3**, we determine K_R and K_L such that $K_R \simeq S_0(1 + \frac{1}{2}\sigma_{ATM}\sqrt{T})$ and $K_L \simeq S_0(1 - \frac{1}{2}\sigma_{ATM}\sqrt{T})$, where σ_{ATM} is the ATM implied volatility for each case.

2. $A_L = \tilde{f}(0)$ for **Case 1**. As for **Case 2** and **Case 3**, A_L is approximately equal to the absorption density obtained by (b) the fifth order expansion or (c) the third order expansion.
3. As for the parameter $\tilde{\sigma}$ appearing in $\chi(x)$ for the domain of $[K_R, +\infty)$, we set $\tilde{\sigma} = 0.45$ for **Case 1**, and $\tilde{\sigma} = 0.12$ for **Case 2** and **Case 3**, which is the same level as the implied volatility around the strike price K_R .
4. γ and A_R is determined so that χ is continuous.

³The frequency of the determination of K_L and K_R is the same as how often the original approximation method should be examined, for instance when the market drastically changes and otherwise once a day. We do not need any additional timing specific to the calibration of K_L and K_R .

In computation we discretize the domain $[0, 4S_0)$ uniformly with 400 grids, where S_0 is the initial underlying asset price. We also use 200 grids for coarser discretization case.

Finally, we set N , the number of the iteration appearing in **4** of **Procedure** in Section 3.3 as:

$100 \times$ (the number of the conditions r in Eq.(3.10)),
or $50 \times$ (the number of the conditions r in Eq.(3.10)).

4.2 Result

In Table 2 - 4 and Figure 1- Figure 6, we report the results for options values expressed as the implied volatilities based on the three parameter sets in Table 1.

Firstly, in Table 2 and Figure 1 of **Case 1**, that is the shorter maturity case $T = 1$, we note that comparing to the third and fifth order expansions ((**b**), (**c**)), our method improves the accuracies for the deep OTM prices, especially in the third order expansion. Moreover, the examination of the left tail of the corresponding density in Figure 5 shows that our nonnegative density approximation is able to take the absorption barrier at $S_T = 0$ into consideration, at least to a certain extent, which cannot be achieved by the original asymptotic expansion method only: the asymptotic expansion itself puts nonzero densities on some negative values of the underlying asset prices.

Next, we report the longer maturity case $T = 10$ in Table 3 and Figure 2. Again, our method whose results appears as the columns of (d1)-(a), (d2)-(a), (e1)-(a), (e2)-(a) in the table generally improves the accuracies for the option prices at the deep OTM. This fact is due to the improvement of the densities, which is observed in Figure 6: for example, our scheme corrects the negative densities as well as the nonzero densities for the negative prices in the fifth order expansion.

Furthermore, let us make some comments on the direct comparison to [4] by using Table 4, Figure 3 and Figure 4, the result for the same parameter set as in Figure 4 of [4]. Here, in the columns of (f1)-(a), (f2)-(a), (g1)-(a), (g2)-(a), we also report the result by our method that includes the information on the estimate of the absorption probability of $S_T = 0$ to \mathcal{K} in (3.5) through its inner product expression.

Although the precise comparison is not possible since the result of [4] is reported only as the graph, it is observed that at least our method with the fifth order expansion provides a better result from $K=1.0\%$ to $K=12\%$, especially much better between $K=2.0\%$ and $K=10\%$ including $K=ATM=4.88\%$. We expect the reason as follows. The first approximate density (2.2) in [4] does not satisfy the conditions that the total mass of the approximate density should be one and that the average of the underlying asset price should be equal to the forward price. (The former condition corresponds to (1) in **Property 1**(*Density Condition*), and the latter to (3) in **Property 2**(*Calibration Condition*) in Section 2 of our paper.) Therefore, the further adjustment (2.13) and (2.14) (in [4]) must be made, which seems ad hoc and does not work very well.

On the other hand, according to Figure 3 in [4], its method seems to work very well for the shorter maturity $T = 1$ as ours. Hence, for the longer maturity our method has an advantage in terms of accuracy. In sum, the main improvement of our scheme is to achieve the systematic and consistent treatment of the conditions that should be satisfied in the probability densities.

We remark that while this experiment shows that it is successful to correct the negative densities and the nonzero densities for the negative rates in the asymptotic expansion, our scheme can be applied to the approximate density of [4] for its further improvement, too.

Moreover, the comparison between the result of 400 grids with 100 iterations and that of 200 grids with 50 iterations in Table 3 and Table 4 shows that our scheme is robust to the coarser discretization and less number of iterations. In fact, the accuracies are almost the same for the parameter sets.

Next, let us report the examples of the computational speed for our scheme. The most part of the computational cost comes from the implementation of the Dykstra's algorithm. For instance, in **Case 3**, based on the machine, Intel(R) Core(TM) i7-3517U @ CPU 1.90GHz \times 2, RAM 4GB, the total computational time with 400 grids and 100 iterations is 0.0845 seconds for one option, 0.0864 seconds for 10 options and 0.1053 seconds for 100 options while the computational time with 200 grids and 50 iterations is 0.0170 seconds for one option, 0.0175 seconds for 10 options and 0.0224 seconds for 100 options. It is almost the

same in the other cases. Thus, combined with the robust result for the coarser discretization and less number of iterations, it seems that the computational speed of our scheme has no problem for practical purpose.

On the other hand, (a) the benchmark Monte Carlo simulation is implemented with 100,000 paths and 365 time steps per year, and the computational time is 104 seconds per one option. Clearly, our scheme is much faster than the benchmark Monte Carlo.

Finally, we remark on a practical application of our scheme. That is, a typical procedure is as follows:

1. Firstly, by using an appropriate analytic approximation formula, we determine the model parameters through calibration to a (reliable) set of market option prices.
2. Given the parameters, we apply our improvement scheme to obtain a no-arbitrage density, which generates reasonable option prices of all the strikes with preserving the previous calibration result.
3. Then, we use this density to evaluate options whose market prices are unquoted or unreliable (as in deep-OTM/ITM options).

We note that the computational time in our scheme is fast enough for this purpose. In this example, as the asymptotic expansion method itself is a closed form approximation, the computational time is only 2.4×10^{-6} seconds per option, that is 0.0024 ms cpu time for 1 option and 0.24 ms cpu time for 100 options, which is fast enough for the calibration purpose. As reported above, our scheme adds very few computational costs.

Case	S_0	σ_0	ε	ρ	T
1.	100	5.00	0.3	-0.5	1
2.	100	1.58	0.3	-0.5	10
3.	4.88%	0.026	0.4	-0.1	10

Table 1: Parameter Set

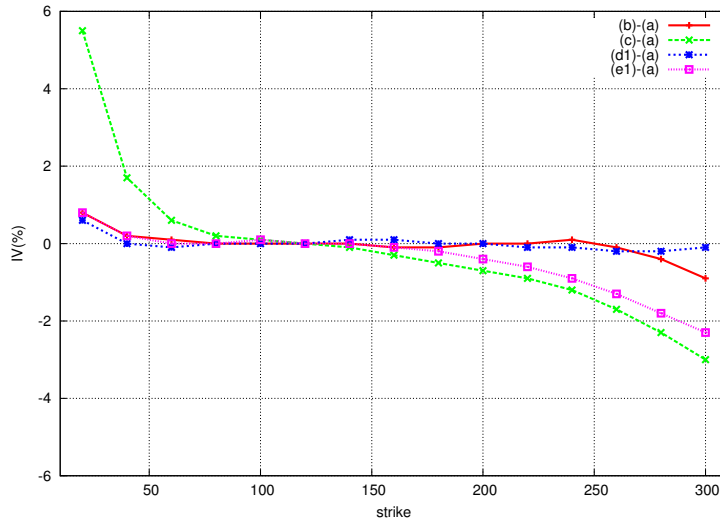


Figure 1: (Case 1, Table 2) Error in IV (%) under SABR model with $c = \frac{1}{2}$ and $T = 1$

strike	(a) IV %	(b)-(a)	(c)-(a)	(d1)-(a)	(e1)-(a)
20	86.2	0.8	5.5	0.6	0.8
40	69.7	0.2	1.7	0.0	0.2
60	60.5	0.1	0.6	-0.1	0.0
80	54.4	0.0	0.2	-0.0	0.0
100	49.8	0.0	0.1	0.0	0.1
120	46.3	0.0	-0.0	0.0	-0.0
140	43.6	-0.0	-0.1	0.1	-0.0
160	41.4	-0.1	-0.3	0.1	-0.1
180	39.6	-0.1	-0.5	0.0	-0.2
200	38.1	-0.0	-0.7	-0.0	-0.4
220	36.9	0.0	-0.9	-0.1	-0.6
240	36.0	0.1	-1.2	-0.1	-0.9
260	35.3	-0.1	-1.7	-0.2	-1.3
280	34.7	-0.4	-2.3	-0.2	-1.8
300	34.3	-0.9	-3.0	-0.1	-2.3

Table 2: (Case 1, Figure 1) Implied Volatility(IV) (%) under SABR model with $c = \frac{1}{2}$ and $T = 1$
(a) Monte Carlo, (b) 5th order Asymptotic Expansion (5th AE), (c) 3rd order Asymptotic Expansion (3rd AE),
(d1) with 5th AE, (400,100),
(e1) with 3rd AE, (400,100),

(Remark)

1. “(b)-(a)”stands for the deviation % of IV by (b) from IV by (a).
2. “with 5th (3rd) AE, (400,100)” means that the fifth (third) order asymptotic expansion is used in our scheme with 400 grids and 100 iterations.

Strike	(a) IV%	(b)-(a)	(c)-(a)	(d1)-(a)	(d2)-(a)	(e1)-(a)	(e2)-(a)
20	34.5	1.8	10.8	0.4	0.4	3.0	2.9
40	26.4	0.5	4.6	0.1	0.1	2.3	2.3
60	21.5	0.3	2.2	0.2	0.2	1.8	1.8
80	18.1	0.2	1.0	0.3	0.3	1.0	1.1
100	15.6	0.2	0.5	0.3	0.4	0.6	0.7
120	14.0	0.2	0.2	0.3	0.5	0.3	0.4
140	13.2	0.3	-0.1	0.5	0.7	0.1	0.3
160	12.8	0.5	-0.4	1.0	1.3	-0.0	0.4
180	12.8	0.3	-0.4	1.6	1.8	0.4	0.9
200	13.0	-0.9	-0.3	1.9	2.0	1.0	1.3
220	13.2	-3.9	-0.4	1.9	2.0	1.3	1.5
240	13.4	-	-0.7	1.7	1.8	1.3	1.5
260	13.6	-	-1.3	1.5	1.5	1.2	1.3
280	13.8	-2.0	-2.0	1.1	1.1	0.9	1.0
300	14.0	-1.3	-2.8	0.6	0.6	0.5	0.5

Table 3: (Case 2, Figure 2) Implied Volatility (IV) (%) under SABR model with $c = \frac{1}{2}$ and $T = 10$
(a) Monte Carlo, (b) 5th order Asymptotic Expansion (5th AE), (c) 3rd order Asymptotic Expansion (3rd AE),
(d1) with 5th AE, (400,100), (d2) with 5th AE, (200,50),
(e1) with 3rd AE, (400,100), (e2) with 3rd AE, (200,50)

(Remark)

1. “(b)-(a)” stands for the deviation % of IV by (b) from IV by (a).
2. “with 5th (3rd) AE, (400,100) ((200,50))” means that the fifth (third) order asymptotic expansion is used in our scheme with 400 (200) grids and 100 (50) iterations.
3. “-” in the column “(b)-(a)” means a failure in calculation of an implied volatility for the 5th AE due to a negative option price.

Strike	(a) IV%	(b)-(a)	(c)-(a)	(d1)-(a)	(d2)-(a)	(e1)-(a)	(e2)-(a)	(f1)-(a)	(f2)-(a)	(g1)-(a)	(g2)-(a)
0.1%	52.9	-	40.7	-1.6	-2.1	-3.9	-3.3	-0.1	-0.1	-0.1	-0.1
1.0%	29.9	11.5	8.0	-0.5	-0.8	-2.2	-1.8	0.0	0.0	0.1	0.1
2.0%	22.0	0.7	5.0	0.2	0.2	0.0	0.2	0.2	0.2	1.0	1.0
3.0%	17.2	-0.0	2.7	0.1	0.1	1.3	1.4	0.1	0.1	1.6	1.6
4.0%	14.1	0.4	1.2	0.5	0.6	1.2	1.2	0.5	0.6	1.2	1.2
5.0%	12.6	0.3	0.6	0.8	1.1	0.7	0.8	0.8	1.1	0.7	0.8
6.0%	12.5	0.3	0.6	0.6	0.8	0.8	0.9	0.6	0.8	0.8	0.9
7.0%	13.1	0.1	0.8	0.4	0.5	0.1	0.2	0.4	0.5	0.1	0.2
8.0%	13.9	1.0	0.2	0.1	0.2	-0.9	-0.8	0.1	0.2	-0.9	-0.8
9.0%	14.7	2.9	-1.3	-1.0	-1.0	-1.9	-1.8	-1.0	-1.0	-1.9	-1.8
10.0%	15.4	3.1	-3.2	-2.1	-2.1	-2.7	-2.7	-2.1	-2.1	-2.7	-2.7
11.0%	16.0	1.1	-5.0	-3.0	-3.0	-3.5	-3.5	-3.0	-3.0	-3.5	-3.5
12.0%	16.5	-1.6	-6.6	-3.7	-3.7	-4.2	-4.2	-3.7	-3.7	-4.2	-4.2
13.0%	17.1	-4.1	-8.0	-4.4	-4.4	-4.8	-4.8	-4.4	-4.4	-4.8	-4.8
14.0%	17.5	-6.2	-9.2	-5.1	-5.1	-5.4	-5.4	-5.1	-5.1	-5.4	-5.4

Table 4: (Case 3, Figure 3,4) Implied Volatility (IV) (%) under SABR model with $c = \frac{1}{2}$ and $T = 10$
(a) Monte Carlo, (b) 5th order Asymptotic Expansion (5th AE), (c) 3rd order Asymptotic Expansion (3rd AE),
(d1) with 5th AE, (400,100), (d2) with 5th AE, (200,50),
(e1) with 3rd AE, (400,100), (e2) with 3rd AE, (200,50),
(f1) with 5th AE, absorption probability, (400,100), (f2) with 5th AE, absorption probability, (200,50),
(g1) with 3rd AE, absorption probability, (400,100), (g2) with 3rd AE, absorption probability, (200,50)

(Remark) This parameter set is the same as in Figure 4 of [4].

1. "(b)-(a)" stands for the deviation % of IV by (b) from IV by (a).
2. "with 5th (3rd) AE, (400,100) ((200,50))" means that the fifth (third) order asymptotic expansion is used in our scheme with 400 (200) grids and 100 (50) iterations.
3. "with 5th (3rd) AE, absorption probability, (400,100) ((200,50))" means that the fifth (third) order asymptotic expansion and the absorption probability at $S_T = 0$ estimated in advance by Monte Carlo are used in our scheme with 400 (200) grids and 100 (50) iterations.
4. The total computational time with 400 grids and 100 iterations is 0.0845 seconds for one option, 0.0864 seconds for 10 options and 0.1053 seconds for 100 options, while the computational time with 200 grids and 50 iterations is 0.0170 seconds for one option, 0.0175 seconds for 10 options and 0.0224 seconds for 100 options. (The result is based on the machine, Intel(R) Core(TM) i7-3517U @ CPU 1.90GHz \times 2, RAM 4GB.)
5. "-" in the column "(b)-(a)" means a failure in calculation of an implied volatility for the 5th AE due to a negative option price.

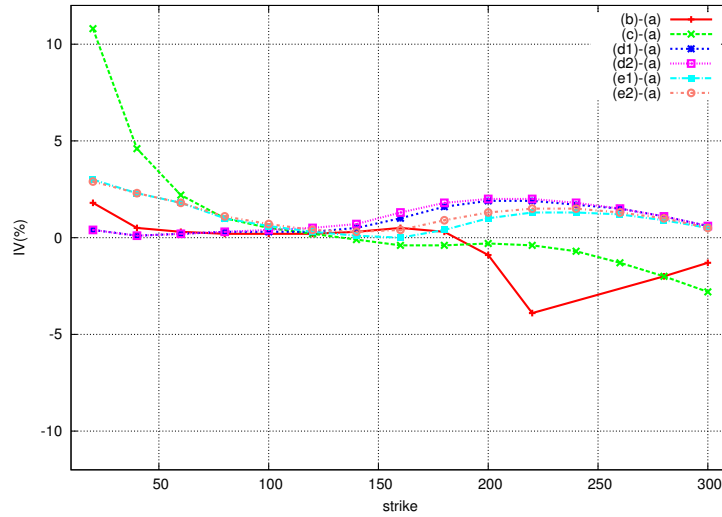


Figure 2: (Case 2, Table 3) Error in IV (%) under SABR model with $c = \frac{1}{2}$ and $T = 10$

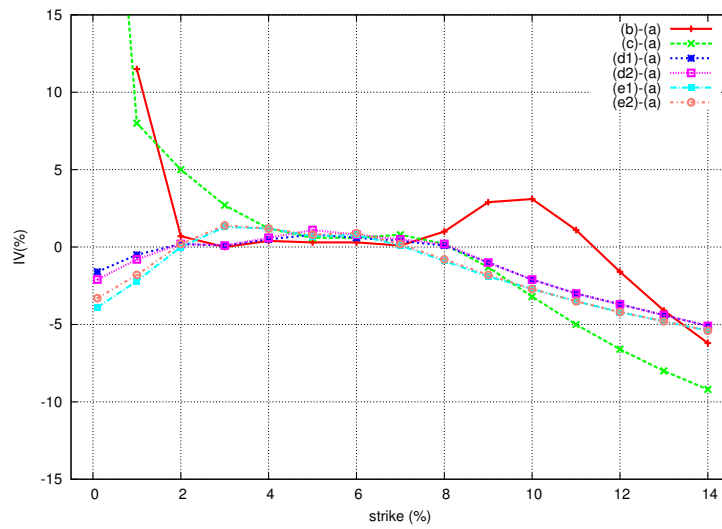


Figure 3: (Case 3, Table 4: (b)-(e2)) Error in IV (%) under SABR model with $c = \frac{1}{2}$ and $T = 10$

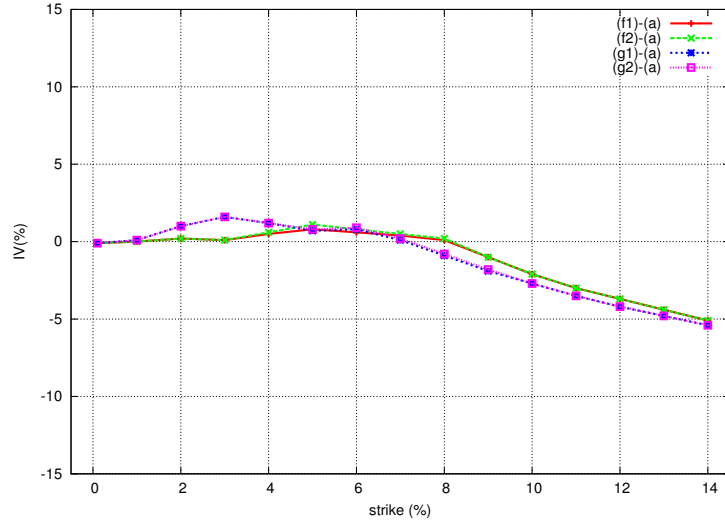


Figure 4: (Case 3, Table 4: (f1)-(g2)) Error in IV (%) under SABR model with $c = \frac{1}{2}$ and $T = 10$

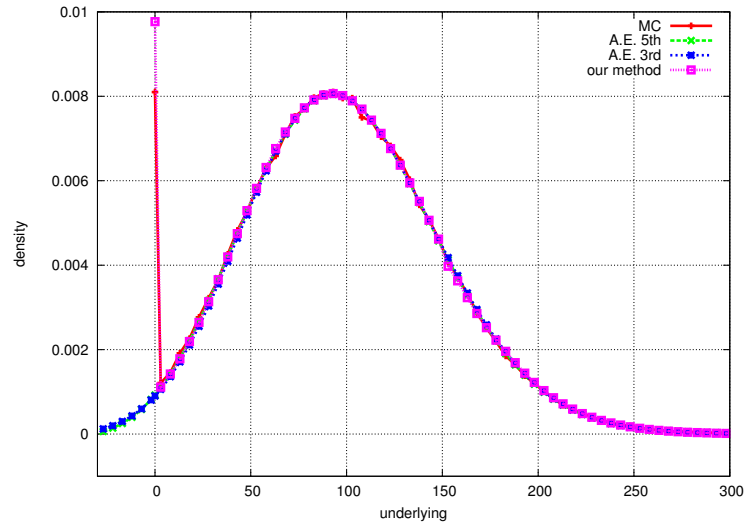


Figure 5: (Case 1) Densities under SABR model with $c = \frac{1}{2}$ and $T = 1$ (our method: (d1) with 5th AE)

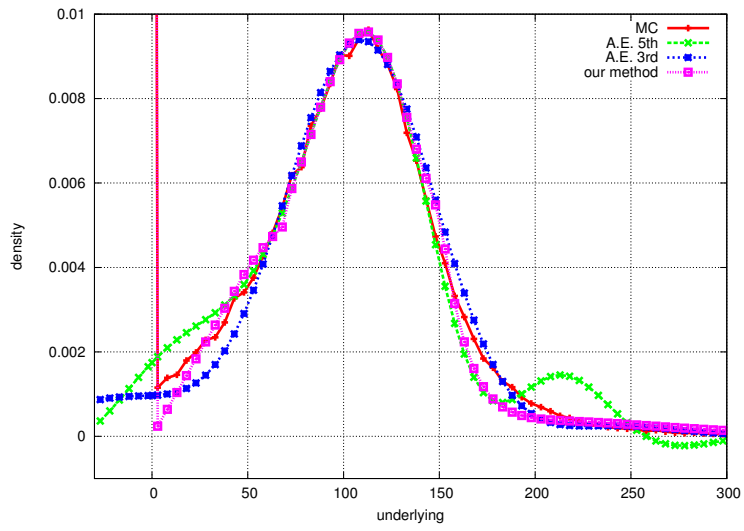


Figure 6: (Case 2) Densities under SABR model with $c = \frac{1}{2}$ and $T = 10$ (our method: (d1) with 5th AE)

5 Conclusion

We have proposed a novel method inspired by the Hilbert space projection theorem for improving an arbitrary density approximation. Particularly, applying the so called *Dijkstra's cyclic projections algorithm*, we are easily able to implement it in practice with market data such as option prices with strikes used for usual calibration.

In the method, we start with an arbitrary approximate density, and then improve the density to meet a set of conditions such as **Property 1**(*Density Condition*) in Section 2 that should be satisfied by density functions. In addition, our method is able to create a new approximate density that has certain desirable properties in practice such as described in **Property 2**(*Calibration Condition*). Also, the method enable the new density to satisfy any conditions that one would like to put on an approximate density such as **Property 4**(*Weak Tail Condition*). In this way, we have achieved the improvement of an approximation, whatever a starting approximate density is.

Moreover, numerical experiments under SABR model have demonstrated the validity of the method. For instance, in terms of the approximation accuracy, this scheme improved the third and fifth order asymptotic expansions with few additional computational costs, preserving the required conditions for the approximate density such as non-negativity and the total mass being one. In addition, it was observed that the improved densities generally provided more precise approximation of option values.

It could be stressed that the method is general and flexible enough to include any conditions and information on an arbitrary approximate density. Further, estimates of the absorption probabilities based on Monte Carlo simulations as in [4] can be consistently plugged into our method. More concrete and detailed examinations on those features will be one of our future research topics.

References

- [1] Bayer, C., and Laurence, P., [2012], *Asymptotics beats Monte Carlo: The case of correlated local vol baskets*, preprint, forthcoming in *Communications on Pure and Applied Mathematics*.
- [2] Benaim, S., Friz, P. and Lee, R. [2008], "On Black-Scholes Implied Volatility at Extreme Strikes," In "Frontiers in Quantitative Finance: Volatility and Credit Risk Modeling," (Cont, R. ed.), Wiley, 2008.
- [3] Deutsch, F. [2001], "Best Approximation in Inner Product spaces," Springer, New York, 2001.
- [4] Doust, P. [2012], *No-arbitrage SABR*, *The Journal of Computational Finance*, Vol. 15, No. 3, Spring 2012.
- [5] Fouque, J. P., G. Papanicolaou and K. R. Sircar [2000], *Derivatives in Financial Markets with Stochastic Volatility*, Cambridge University Press.
- [6] Gatheral, J., Hsu, E.P., Laurence, P., Ouyang, C. and Wang, T-H.[2009], "Asymptotics of implied volatility in local volatility models," *Mathematical Finance*, 22(4), 2012, 591-620.
- [7] Hagan, P.S., Kumar, D., Lesniewski, A.S., and Woodward, D.E. [2002], *Managing Smile Risk*, *Wilmott Magazine*, 2002, 84-108.
- [8] Lee, R. [2004], "The Moment Formula for Implied Volatility at Extreme," *Mathematical Finance*, 14(3): 469-480.
- [9] Shiraya, K., Takahashi, A. [2011], *Pricing Average Options on Commodities*, *Journal of Futures Markets*. Vol.31-5, 407-439, 2011.
- [10] Shiraya, K., Takahashi, A. [2012], *Pricing Multi-Asset Cross Currency Options*, *Journal of Futures Markets*, Vol.34-1, 1-19, January., 2014.
- [11] Siopacha, M. and Teichmann, J. [2011], "Weak and Strong Taylor Methods for Numerical Solutions of Stochastic Differential Equations," *Quantitative Finance*, Volume 11-4, 517-528, 2011.
- [12] Takahashi, A. [1999], *An Asymptotic Expansion Approach to Pricing Contingent Claims*, *Asia-Pacific Financial Markets*, Vol. 6, 1999, 115-151.
- [13] Takahashi, A., Takehara, K. and Toda. M. [2012], *A General Computation Scheme for a High-Order Asymptotic Expansion Method*, *International Journal of Theoretical and Applied Finance*, 15(6), 2012.